Macromolecules
ARTICLE

Macromolecules **2010**, *43*, 827–836 **827**
DOI: 10.1021/ma9018747

Solvent Effects on Free Radical Polymerization Reactions: The Influence of Water on the Propagation Rate of Acrylamide and Methacrylamide

Bart De Sterck,[†] Roel Vaneerdeweg,[†,§] Filip Du Prez,[‡] Michel Waroquier,[†] and Veronique Van Speybroeck*,[†]

[†]*Center for Molecular Modeling, Ghent University, Technologiepark 903, B-9052 Zwijnaarde, Belgium, QCMM-alliance, Ghent-Brussels, Belgium and* [‡]*Department of Organic Chemistry, Polymer Chemistry Research Group (PCR), Ghent University, Krijgslaan 281 S4-bis, B-9000 Ghent, Belgium.* [§]*Current address: Departement LNE, Afdeling Milieu-inspectie (hoofdbestuur), Koning Albert II-laan 20 bus 8, 1000 Brussels, Belgium*

Received August 23, 2009; Revised Manuscript Received October 30, 2009

ABSTRACT: The polymerization of acrylamide (AA) and methacrylamide (MAA) was studied by an extensive set of computational methods with a particular focus on the possible influence of water molecules on the propagation reaction. An extensive set of electronic structure methods was tested, consisting of B3LYP, BMK, MPWB1K, MP2, and B2-PLYP of which some include dispersion effects. The effect of water on the transition state is modeled in two different ways. Explicit water molecules are added to the system, showing that replacing the hydrogen bond that dominates the transition state structure by a water-mediated hydrogen bond, results in more stable, more feasible transition states. This effect is the largest for AA polymerization, a monomer that is known to experience a larger solvent effect than MAA. Additionally, a conductor-like polarizable continuum model (C-PCM) is applied on both the transition states in gas phase and the ones bearing explicit water molecules. This model has a dramatic effect on all the propagation rates, raising them by about 3 orders of magnitude. The inclusion of explicit water molecules gives insight into the role of water molecules and the formation of prereactive complexes. The relative rate of polymerization of AA with regard to MAA is well reproduced for a trimeric propagating radical with inclusion of explicit water molecules or by using an implicit solvation model at the BMK and MPWB1K level of theory.

Introduction

Free radical polymerization is one of the most important reaction mechanisms for the industrial production of a wide variety of polymers. It is a complex multistep process and the determination of rate coefficients of the various elementary reactions is a challenge both for theoreticians and experimentalists. From the experimental point of view, substantial progress has been made since the establishment of elegant laser-flash photolysis-based techniques, such as pulsed laser polymerization (PLP) and time-resolved PLP. Computational quantum chemistry has the potential to study individual reactions and their rates without kinetic model-based assumptions. However the modeling of radical reactions generally requires high levels of theory which are not feasible for polymeric systems. Nonetheless, due to a continuing increase in computer power and the development of advanced numerical models, computational chemistry has established itself as a useful tool for the radical polymer field. In the literature, a rich database exists consisting of both experimental[1−5] and theoretical data for a broad range of radically polymerizing monomers like ethylene,[6,7] (meth)acrylate-type monomers,[8−10] styrene,[11] (meth)acrylamide-type monomers, acrylonitrile,[12] and vinyl chloride.[13]

To date, there have been relatively few published direct assessments of the influence of solvent on radical reactions. Moreover, experimental solvation energies for radical species are scarce in the literature. However, as some polymerizations are carried out in solution, the knowledge of the effects that are induced by the solvent is crucial for a better understanding of free radical polymerization in solution. Therefore, theoretical modeling of the kinetics of propagation reactions should take solvent effects into account. It has long been recognized that solvents may affect the reaction kinetics but the origin of the solvent effect and the extent of its influence have been the onset of a long debate. Reaction rate coefficients (k_p) for styrene and methyl methacrylate (MMA) polymerizations have been measured in a wide variety of solvents by Olaj et al.[14] and the solvent-induced changes were found to vary around 20%. In other experimental work, one notices a significant increase in k_p in some specific polar solvents when the monomer concentration decreases. Recently Beuermann published a very good review on the current status of the solvent influence on the propagation kinetics studied by pulsed laser initiated polymerizations.[15] Various effects may contribute to changes in k_p due to solvent such as hindered rotational modes, hydrogen bonding[16] or electron/pair interactions. These may lead to an enhancement of a factor 10 of the propagation rate. In contrast, nonspecific solvent interactions originating from solvent size, local monomer concentration or steric effects lead to less pronounced variations in k_p.[16]

In this article, attention is focused on two polar monomers, i.e., acrylamide (AA) and methacrylamide (MAA), for which specific interactions between solvent and monomer occur through hydrogen bonding. In aqueous solution, the concentration of a monomer that is prone to hydrogen bonding will influence the reaction rate and the Arrhenius parameters compared to bulk polymerization.[17−19] This was observed for a variety of polar monomers like acrylamide (AA),[20,21] methacrylamide (MAA),[22] *N*-isopropylacrylamide (NIPAM),[23] acrylic acid,[24,25] and methacrylic acid.[26] These effects are often ascribed to the reversible formation of prereactive complexes. In the literature, complexation between radical and monomer[23,27−29] as well as radical-solvent interaction[17] is

*To whom correspondence should be addressed. E-mail: veronique.vanspeybroeck@ugent.be.

Published on Web 12/31/2009

Scheme 1. Schematic Representation of Different Chain Lengths for Syndiotactic Propagation of Acrylamide (R = H) and Methacrylamide (R = Me)

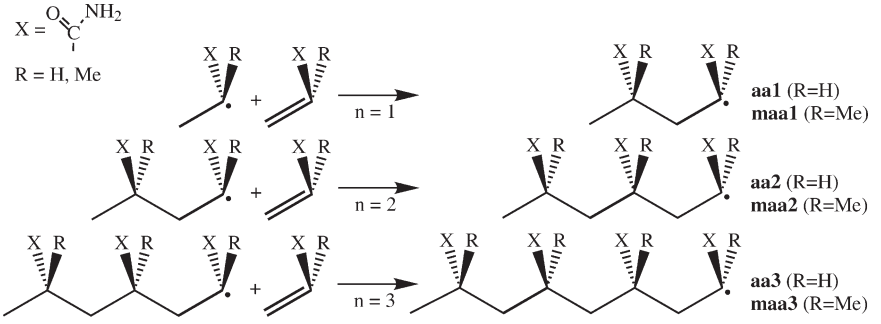

proposed. For the studied system, the polymerization of acrylamide, similar experimental findings and hypotheses are well documented. Several pulsed laser polymerization studies (PLP) clearly show that AA polymerization exhibits a strong solvent effect in aqueous solution.[21,28−30] The class of acrylamides, methacrylamides, and derived monomers have always been interesting monomers for a wide range of applications, for instance for the ability of the corresponding polymer hydrogels to absorb huge amounts of water.[31] These gels have applications ranging from analysis (gel electrophoresis)[32] to nanotechnology.[33] An acrylamide-derived monomer such as NIPAM is one of the most studied monomers as a result of its peculiar lower critical solution behavior. Several studies on the solvation of acrylamide have shown that acrylamide exists as a hydrogen-bonded complex with one or more water molecules.[34,35] This interaction will certainly play a role in the behavior of the reacting monomers and should be incorporated in the molecular model in order to completely account for them in the evaluation of the propagation reaction rate coefficients. An other aspect of acrylamide solvation is the result of the presence of the hydrophobic vinyl bond. Although this entity will not interact directly with the water molecules, an electrostatic effect of the surrounding dipolar water molecules can not be neglected.[36] This is certainly the case for methacrylamide which has a second hydrophobic group.

Until now, the majority of quantum chemical studies on radical polymerizations have been carried out in the gas phase. Gas phase predictions for polymerization in a solvent environment where explicit solvent interactions occur systematically underestimate the propagation reaction rate constants k_p in density functional theory (DFT) methods even if the most advanced functionals are used. More recently, some studies appeared in which the solvent was treated implicitly by a polarizable continuum model. These studies showed that the continuum solvation model is capable of capturing a substantial amount of the solvation effects.[21,29] These models show a minor effect on the polymerization of acrylonitrile and vinyl chloride in toluene, tetrahydrofuran and dimethylformamide[37] and a large (10.5 kJ·mol^{-1}) decrease in activation energy for acrylic acid in water.[38] However, in the case where the solvent effect is mainly due to hydrogen bonding, these models fail as it was shown for the ethyl α-hydroxymethacrylate (EHMA) system for which the gap between experiment and theory increased by 3 orders of magnitude upon inclusion of a continuum solvation model.[8]

In this article, we will evaluate the influence of solvent effects on the propagation rate of acrylamide and methacrylamide. Therefore, we will not only assess the influence of a dielectric continuum on the reaction rate, but we will also take into account explicit water molecules assisting the transition state. Embedding these molecular clusters in the continuum model is often referred to as the supermolecule method, the cluster-continuum method or the mixed implicit/explicit solvent model.[39,40] Although the determination of the amount and the location of the explicit solvent molecules is not always trivial (one should only include the relevant solvent molecules that strongly interact with the solute),[41,42] this model has proven to be very useful in reaction and solvation modeling. A comparative study of continuum, explicit and mixed solvation models has been performed for studying phosphate hydrolysis by the group of Warshel.[42] It turned out that the mixed implicit/explicit solvation model gave unreliable results if the number of explicit solvent molecules became too large or if the solvent molecules do not show the correct orientation. In this work we tested the adequacy of the three solvation models on the radical polymerization systems. In particular the effect of explicit water molecules on the structures, energies and kinetic parameters for the polymerization of AA and MAA will be investigated combined with a continuum model or not.

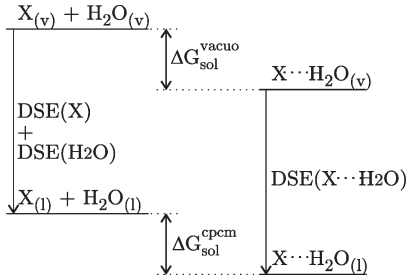

Figure 1. Thermodynamic cycle for the determination of the free energy of solvation of a solute, X, in a dielectricum (ΔG_{sol}^{cpcm}), calculated from the free energy of solvation in vacuo (ΔG_{sol}^{vacuo}) and the dielectric solvation energies (DSEs).

Computational Methods

Rate coefficients, Arrhenius parameters, solvation energies and Gibbs free energies were calculated for the propagation reaction of two monomers, namely acrylamide (AA) and methacrylamide (MAA). In each case, transition states for reaction with a monomeric (**aa1**, **maa1**), dimeric (**aa2**, **maa2**), and trimeric (**aa3**, **maa3**) radical were used as a model for growing polymer so as to investigate the chain length effect on the propagation rate. These models are shown in Scheme 1. Notice that only syndiotactic propagation will be considered in this paper as the main scope is to understand how water molecules can interact with the transition state and influence the reaction kinetics.

Several studies have shown a rapid rate of convergence of the kinetic coefficients with respect to the chain length.[10,37,43−45] Notice that it is very important to start with an analogous series of reactants and transition states. Considering the higher flexibility of the longer radicals, it is important to use configurationally similar structures for all the reactions considered. This can be seen in Scheme 1 for the reactions in gas phase.

The effect of the solvent, water, is modeled as the sum of two contributions (see Figure 1): one resulting from the coordination of one or more water molecules to the transition state (X) and one originating from the bulk solvent effect.[39,46−49] The first contribution is the free energy of solvation in vacuo (ΔG_{sol}^{vacuo}) and

accounts for the effect of hydrogen bonds that can assist the radical addition reaction while the second contribution essentially takes into account the permanent dipole moment of the surrounding water molecules by placing the transition state in a dielectric continuum, resulting in a dielectric solvation energy (DSE). For the latter effect, single point energy calculations using the C-PCM model as implemented in Gaussian03 is used with Pauling radii for the solute.[50,51] Combination of both contributions allows us to calculate the coordination free energy in solution, ΔG_{sol}^{cpcm}, from the thermodynamic cycle that is depicted in Figure 1.

Full geometry optimizations for transition states and stable minima are performed with DFT using the B3LYP[52,53] density functional. This method is known for it is ability to produce good geometries and it has been used intensively for the modeling of radical reactions. Test calculations with both the 6-31+G(d,p) and the 6-311++G(d,p) basis set show that the geometries undergo very little influence from the basis set.

The results are corrected for the zero-point energy and a normal-mode analysis is performed to ensure that the calculated structures are either a local minimum (no imaginary frequencies) or a transition state (saddle point, 1 imaginary frequency). All DFT optimizations were carried out using the Gaussian03 software package.[51] For the calculation of the kinetic parameters, no scaling factors were used for the frequencies nor for the zero-point energy correction. The kinetic parameters for the reactions in vacuo were calculated by fitting an Arrhenius equation to the calculated values for the reaction rate coefficient between 200 and 400 K. The C-PCM kinetics was calculated using Gibbs free energy of activation.

Additionally, single point energy calculations were carried out for the optimized structures using more advanced electronic structure methods. The following electronic structure methods are used: MPWB1K, BMK, UMP2, and B2-PLYP with the 6-31+G(d,p) basis set using Gaussian03. The MPWB1K method is selected because of its good description of hydrogen bonding, weak van der Waals interaction, partial bonding, and the more accurate thermochemistry results.[10,54] The BMK functional is chosen because of its good performance for describing the kinetics of radical reactions in general.[13,55,56] The effect of higher order corrections is investigated with the UMP2 second order perturbation method, from here referred to as MP2. The B2-PLYP method, which combines the BLYP[53,57] functional with Hartree−Fock exchange and a perturbative second-order correlation part, is used since it is a promising functional with a high accuracy, taking into account dispersion interactions.[58,59]

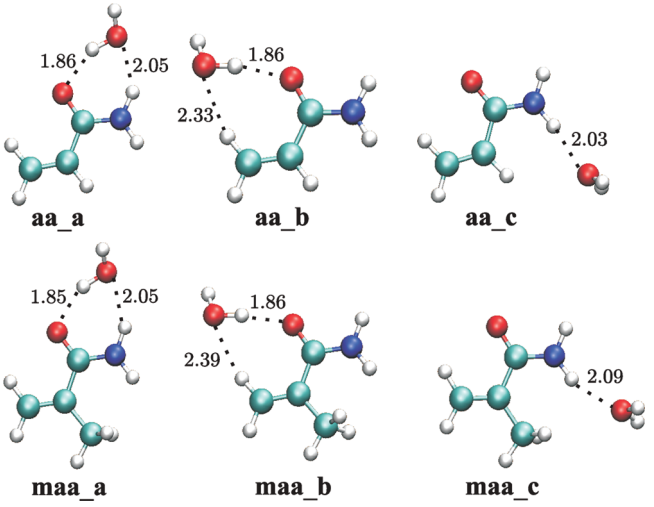

Figure 2. B3LYP/6-31+G(d,p) optimized structures for monosolvated AA and MAA monomers. Distances are in Å.

Table 1. Energies of Solvation for the AA and MAA Monomers Using the B3LYP/6-31+G(d,p) Geometries and Single Point Energy Calculations for a Variety of Electronic Structure Methods[a]

	AA				
	B3LYP	BMK	MPWB1K	MP2	B2PLYP
aa_a	−31.60	−31.30	−34.36	−34.07	−35.41
aa_b	−22.39	−21.59	−23.84	−24.58	−25.71
aa_c	−17.45	−16.70	−19.88	−22.97	−21.40
	MAA				
	B3LYP	BMK	MPWB1K	MP2	B2PLYP
maa_a	−32.03	−31.83	−34.83	−34.65	−36.03
maa_b	−21.39	−20.89	−23.54	−24.26	−24.96
maa_c	−14.35	−13.99	−17.02	−20.46	−18.39

[a] All values are in kJ·mol^{-1}.

Results and Discussion

Solvation. To understand the influence of water molecules on the reaction kinetics, possible solvated structures of the monomers are investigated first. Both monomers feature several sites that are prone to hydrogen bonding, namely the acrylic oxygen atom and the amide hydrogens. Putting a water molecule in the vicinity of these hydrogen bond donors and acceptors, results in 3 conformations for each monomer:

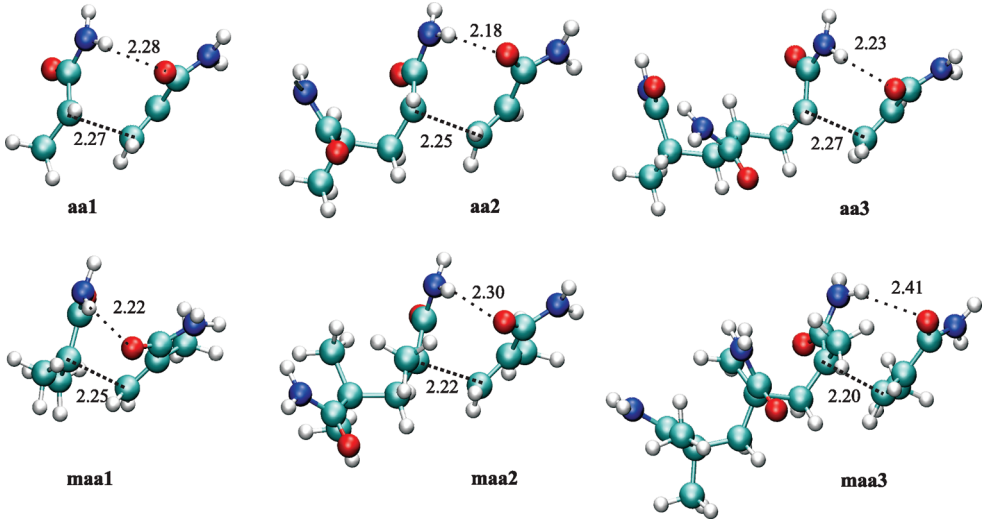

Figure 3. Gas phase transition states for the addition of AA and MAA to a monomeric, dimeric, and trimeric propagating radical.

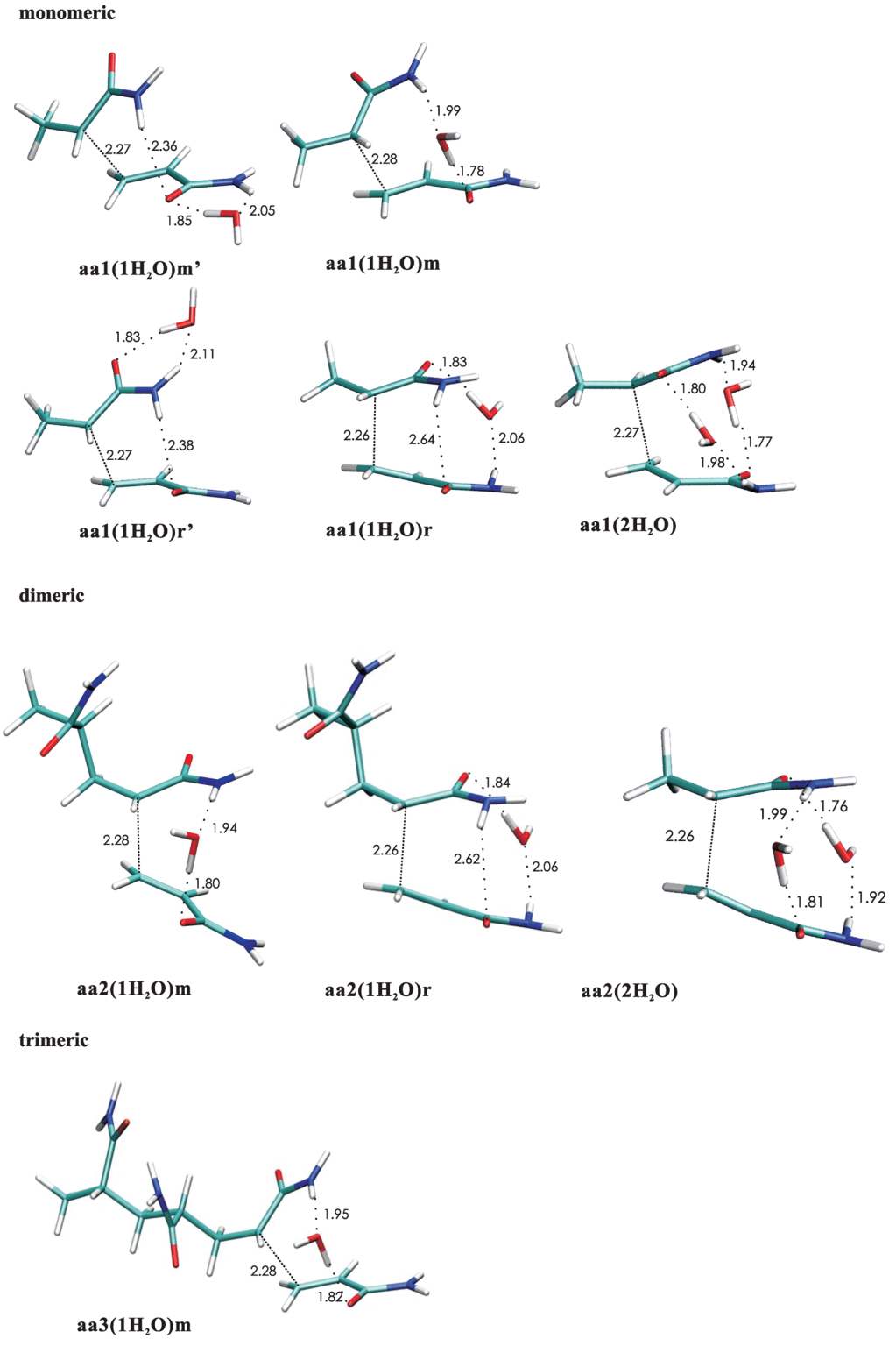

Figure 4. Solvated structures of the AA transition states.

aa_a, **aa_b**, **aa_c** and **maa_a**, **maa_b**, **maa_c**, see Figure 2 and Table 1. Both static and dynamic studies on the solvation of acrylamide in water, performed by Balbuena et.al.,[34,35] show that the acrylamide carbonyl oxygen coordinates with water hydrogen and that the bridge-type interactions **aa_a** and **maa_a** are the most stable. These findings are confirmed here for various electronic structure methods. In the rest of this paper, the water bridge solvated monomers **aa_a** and **maa_a** will be taken as a reference reactant for calculating the energetics of the reactions considered.

Next, the transition state for the addition of the acrylamide (AA) and methacrylamide (MAA) monomer to their respective radicals is investigated. In a first step, geometry optimizations for transition states are performed in the gas phase using the B3LYP/6-31+G(d,p) electronic structure method. Moreover, due to the orientation of both molecules in the most stable transition state *in vacuo* for the syndiotactic attack, intermolecular hydrogen bonding takes place between the acrylic oxygen from the monomer and an amide hydrogen from the radical, as shown in Figure 3. On the same figure, the

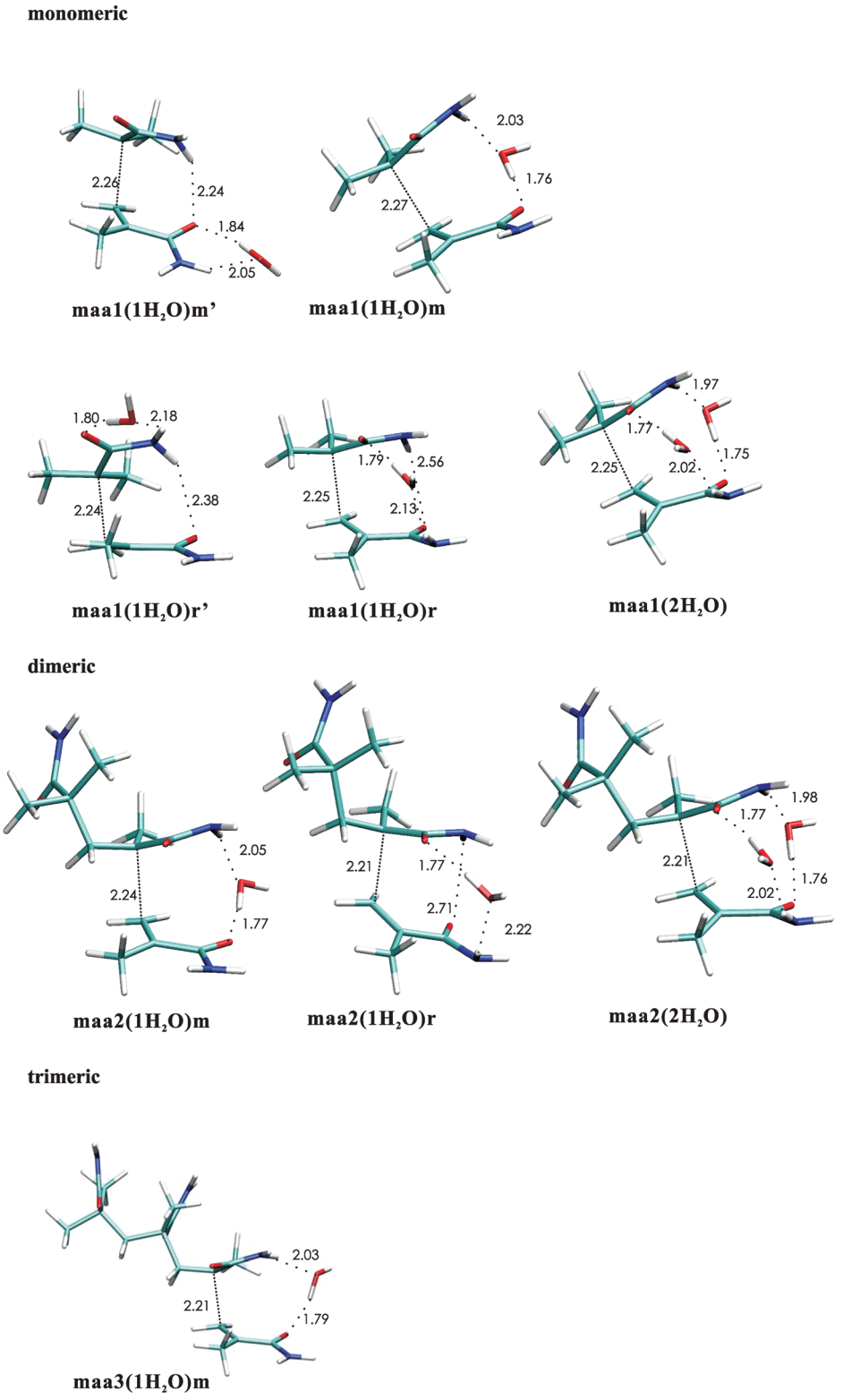

Figure 5. Solvated structures of the MAA transition states.

dimeric and trimeric transition states are also shown for both AA and MAA, and they all show similar characteristics. Rotation of the monomeric transition state about the forming bond does not result in more stable structures, because it would involve breaking of the intermolecular hydrogen bond.

In a next step, solvation of the transition states is studied by explicitly including one or two water molecules to the optimized gas phase geometry and a subsequent reoptimization at the same level of theory. The water molecules were placed around the studied transition states by first identifying the hydrogen bond donors and acceptors in the system. The carbonyl oxygen and the amide hydrogens are the most important sites for interactions with water. Starting with the monomeric transition state, a water molecule was positioned in the vicinity of a hydrogen bond donor or acceptor and the structure was reoptimized to obtain a transition state

Table 2. Gibbs Free Energy (298 K) of Solvation in Vacuo and in the C-PCM Model for the Studied Transition States in the Formation of PAA Using the B3LYP/6-31+G(d,p) Geometries and Single Point Energy Calculations at a Variety of Electronic Structure Methods[a]

	B3LYP		MPWB1K		BMK		MP2		B2PLYP	
	ΔG_{sol}^{vacuo}	ΔG_{sol}^{cpcm}	ΔG_{sol}^{vacuo}	ΔG_{sol}^{cpcm}	ΔG_{sol}^{vacuo}	ΔG_{sol}^{cpcm}	ΔG_{sol}^{vacuo}	ΔG_{sol}^{cpcm}	ΔG_{sol}^{vacuo}	ΔG_{sol}^{cpcm}
aa1(1H$_2$O)m′	5.6	−3.9	2.4	−5.2	6.0	−1.6	1.8	−7.5	1.3	−7.0
aa1(1H$_2$O)r′	2.5	−4.3	−1.4	−6.4	2.4	−2.2	−2.4	−8.7	−1.9	−7.5
aa1(1H$_2$O)m	−2.0	−13.0	−2.8	−11.9	−0.5	−9.0	−7.2	−17.5	−7.3	−16.4
aa1(1H$_2$O)r	4.3	3.9	−1.7	0.5	2.4	4.6	−6.8	−7.4	−4.2	−2.9
aa1(2H$_2$O)	−1.7	−9.4	−9.7	−13.5	−3.1	−6.0	−18.2	−25.4	−15.5	−19.6
aa2(1H$_2$O)m	−3.8	−11.3	−4.1	−11.1	−2.3	−7.7	−10.6	−17.6	−9.6	−15.9
aa2(1H$_2$O)r	3.7	3.9	−1.9	0.4	1.8	4.5	−7.5	−7.5	−4.9	−3.0
aa2(2H$_2$O)	−0.9	−9.1	−8.0	−14.0	−2.5	−6.1	−18.9	−26.5	−15.4	−20.5
aa3(1H$_2$O)m	1.3	−10.3	0.6	−10.1	3.1	−6.7	−6.5	−17.7	−5.1	−15.5

[a] All values are in kJ·mol^{-1}.

Table 3. Gibbs Free Energy (298 K) of Solvation in Vacuo and in the C-PCM Model for the Studied Transition States in the Formation of PAA Using the B3LYP/6-31+G(d,p) Geometries and Single Point Energy Calculations at a Variety of Electronic Structure Methods[a]

	B3LYP		MPWB1K		BMK		MP2		B2PLYP	
	ΔG_{sol}^{vacuo}	ΔG_{sol}^{cpcm}	ΔG_{sol}^{vacuo}	ΔG_{sol}^{cpcm}	ΔG_{sol}^{vacuo}	ΔG_{sol}^{cpcm}	ΔG_{sol}^{vacuo}	ΔG_{sol}^{cpcm}	ΔG_{sol}^{vacuo}	ΔG_{sol}^{cpcm}
maa1(1H$_2$O)m′	6.3	−4.2	4.4	−4.9	7.1	−1.5	2.4	−7.9	2.0	−7.4
maa1(1H$_2$O)r′	4.2	−0.7	−1.2	−4.7	3.4	0.3	−3.7	−8.5	−1.3	−5.1
maa1(1H$_2$O)m	5.6	−7.3	2.1	−10.3	4.1	−7.3	−2.7	−16.0	−1.2	−13.1
maa1(1H$_2$O)r	9.0	25.9	5.5	5.9	7.7	8.8	−1.7	−2.9	0.8	1.4
maa1(2H$_2$O)	4.4	−3.0	−2.4	−8.1	2 2	−1.8	−13.6	−21.3	−10.0	−15.0
maa2(1H$_2$O)m	4.9	−4.2	0.9	−7.8	3.1	−4.6	−5.1	−14.6	−2.8	−11.0
maa2(1H$_2$O)r	9.1	9.5	4.8	6.8	6.8	9.4	−2.7	−2.2	0.4	2.6
maa2(2H$_2$O)	5.9	−3.3	0.0	−7.5	3.9	−1.7	−12.7	−22.0	−8.9	−15.8
maa3(1H$_2$O)m	4.8	−6.4	3.9	−6.6	5.1	−4.7	−0.9	−12.4	−1.2	−11.5

[a] All values are in kJ·mol^{-1}.

with one imaginary frequency. With this procedure, one or two water molecules were added to the system. The resulting structures are compared to each other and the Gibbs free energy of solvation is evaluated with respect to the transition state in vacuo since this number will determine the rate enhancement resulting from the water molecule. The different water positions that are considered at this stage are shown in Figure 4 for acrylamide and in Figure 5 for methacrylamide.

The possible locations of the water molecules are first explained for the monomeric transition state of acrylamide **aa1**. Two different water orientations can be distinguished: nonbridging and bridging solvation. In the former kind, a water molecule coordinates with the propagating monomer (**aa1(1H$_2$O)m′** and **maa1(1H$_2$O)m′**) or radical (**aa1(1H$_2$O)r′** and **maa1(1H$_2$O)r′**). When a water molecule makes a connection between both reactants, it can either replace the existing hydrogen bond by a water bridge (**aa1(1H$_2$O)m** and **maa1(1H$_2$O)m**, the water molecule interacts with the oxygen atom of the monomer) or create a new water bridge at the other side of the structure (**aa1(1H$_2$O)r** and **maa1(1H$_2$O)r**, the water molecule interacts with the oxygen atom of the radical). Analogous sampling for the possible locations of the water molecule were performed for methacrylamide and are shown in Figure 5. For the dimeric and trimeric transition states, the sampling was restricted to bridging structures as they were found to be more stable than the nonbridging geometries. In a further step, single-point C-PCM free energy calculations are performed. This is repeated for a variety of electronic structure methods as outlined in the Computational Details. The Gibbs free energies of solvation for the acrylamide transition states are given in Table 2 for the explicit solvent model (ΔG_{sol}^{vacuo}) and the explicit/implicit solvent model using the C-PCM scheme (ΔG_{sol}^{cpcm}). Table 3 reports the results for methacrylamide.

It is clear that not all the considered positions for water molecules are equally favored. The nonbridging interactions are in general less favorable and therefore, only bridging interactions were considered for the larger chains. The bridging interactions (**aa1(1H$_2$O)m**, **aa2(1H$_2$O)m**, **aa3(1H$_2$O)m** and **maa1(1H$_2$O)m**, **maa2(1H$_2$O)m**, **maa3(1H$_2$O)m**) give rise to the largest negative free energies of solvation, ΔG_{sol}^{cpcm}. This feature is a combined effect from hydrogen bonding and the interaction with the bulk solvent that can be observed over all electronic structure methods studied. Relaxing the intramolecular hydrogen bond also seems to be an incentive for a second water bridge at the other side of the transition state, resulting in negative free energies of solvation for transition states with a double water bridge (**aa1(2H$_2$O)**, **aa2(2H$_2$O)** and **maa1(2H$_2$O)**, **maa2(2H$_2$O)**). For electronic structure methods including dispersion interactions, the total free energy of solvation becomes more negative than with one water molecule. In that case, two water bridges are formed between the monomer and the propagating radical.

The preference to form bridging interactions with water molecules rather than direct hydrogen bonds was calculated before and is important in understanding water-mediated interactions.[60] The free energy decrease means that the presence of the water molecule will increase the reaction rate since the water-assisted transition state is more favorable compared to the gas phase transition state. For the monomeric transition states, the water bridge loosening the intramolecular hydrogen bond is the most favored one and will be considered in the next section. In that section, also dimeric and trimeric structures, with bridging solvation will be considered because that type of interaction will have the most prominent effect on reaction kinetics, as will be shown in the next section.

Reaction Kinetics. In order to determine the reaction rates and kinetic parameters, internal reaction coordinate (IRC) calculations were performed in order to find the reactant and product structures that correspond to each transition state that was selected in the previous section. The gas phase results will be used as a reference point. The IRC calculations

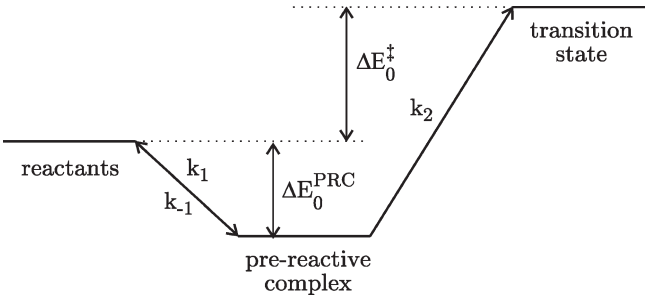

Figure 6. Schematic representation of the role of the prereactive complex in the apparent reaction rate coefficient.

show the existence of prereactive complexes (PRCs) (see Figure 7) and a dimeric, trimeric or tetrameric radical as products. The PRCs are characterized by water molecules forming hydrogen bridges between monomer and radical, but the reactants are not properly aligned to form the carbon−carbon bond.

By considering the PRCs, the apparent kinetic parameters can be split up in two contributions: the unimolecular rate coefficient (k_2) and the equilibrium constant for the formation of the PRC (K_1) as is shown in Figure 6.[61]

$$M + R_m^{\bullet} \underset{k_{-1}}{\overset{k_1}{\rightleftharpoons}} PRC \quad (1)$$

$$PRC \xrightarrow{k_2} R_{m+1}^{\bullet} \quad (2)$$

$$r = k_2[PRC] \quad (3)$$

$$\frac{d[PRC]}{dt} = 0 = -k_2[PRC] + k_1[M][R_m^{\bullet}] - k_{-1}[PRC] \quad (4)$$

$$r = k_{app}[M][R_m^{\bullet}] = \frac{k_1 \times k_2}{k_{-1} + k_2}[M][R_m^{\bullet}] = K_1 k_2 [M][R_m^{\bullet}] \quad (5)$$

$$k_{app} = K_1 k_2 \quad (6)$$

When assuming that the reaction is not diffusion-controlled, the reaction rate can be written as eq 3. The unknown PRC concentration in this equation follows from a pseudo-stationary state hypothesis on these species (eq 4). In eq 5, the factor k_2 in the denominator is smaller than k_{-1} because the reaction is assumed to be kinetically controlled, resulting in the apparent reaction rate coefficient that is shown in eq 6. This also means that calculating the reaction rate from separated reactants will result in exactly the same rate coefficients as compared to calculating the product of the equilibrium constant and the unimolecular reaction rate. Although one could start from the separated reactants, the PRC concept is very valuable to get more insight into the role of the solvent molecules and their ability to stabilize the transition state. In the following the apparent reaction rate coefficient, k_{app}, will be systematically used for the reaction rate constant.

The kinetic parameters for the selected reactions from Table 2 are shown in Table 4 for the polymerization of acrylamide and in Table 6 for the analogous reactions of methacrylamide. The predicted kinetic parameters when

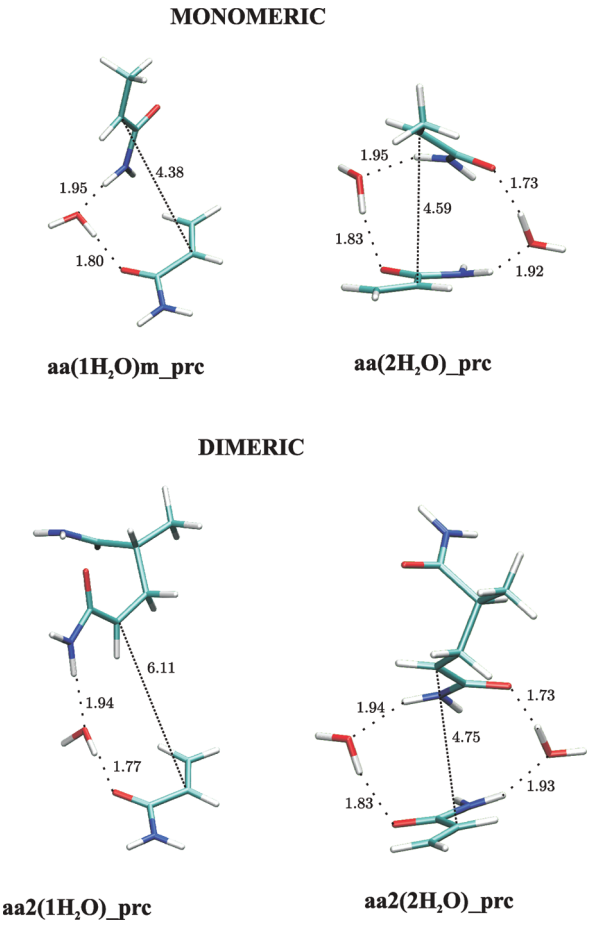

Figure 7. Prereactive complexes for the polymerization of AA.

applying a C-PCM model to the optimized transition states in vacuo are taken up in Table 5 for AA and in Table 7 for MAA.

It a well-known feature and it is confirmed by these calculations that gas phase predictions (**aa1**, **aa2**, **aa3** in Table 4 and **maa1**, **maa2**, **maa3** in Table 6) with standard DFT functionals like B3LYP systematically underestimate the propagation rate constants.[7,62] Choosing other electronic structure methods like BMK, MPWB1K, or B2PLYP can drastically increase the rate constants (k_p), but the propagation rate remains underestimated by at least 2 orders of magnitude, when not accounting for the molecular environment. For the B3LYP functional it is a common feature that reaction barriers are overestimated, yielding unrealistically low absolute values for the reaction rate constants.[37] With BMK—a functional better suited for reproducing kinetics—the k_p values increase with 2 or 3 orders of magnitude, getting closer to the experimental values. Taking dispersion interactions into account with B2PLYP, only small changes are noticed with respect to the BMK predictions: the similarity of the gas phase k_p predictions in both DzaFT methods is striking. The implicit solvation model preferentially stabilizes the transition state, giving rise to a significant increase of 4 orders of magnitude for the reaction rate coefficient in case of AA (Table 5). This drastic enhancement brings some k_p's closer to experiment but for the more advanced electronic methods (MPWB1K, BMK, ...) one gets an overshoot of 2 orders of magnitude. The situation is somewhat different for MAA where the increase is less drastic (Table 7) resulting in a better overall agreement with experiment. It should be noticed, however, that the k_p ratio for AA and MAA polymerization (which is about 75

Table 4. Kinetic parameters for the addition of acrylamide to a monomeric ($n = 1$), dimeric ($n = 2$) and trimeric ($n = 3$) radical chain for different levels of solvation and different electronic structure methods[a]

	B3LYP			MPWB1K		BMK		MP2		B2PLYP	
	A	E_A	k_{298K}	E_A	k_{298K}	E_A	k_{298K}	E_A	k_{298K}	E_A	k_{298K}
						Monomer					
aa1	2.08×10^2	26.3	5.2×10^{-3}	17.0	2.2×10^{-1}	19.5	8.0×10^{-2}	31.8	5.8×10^{-4}	19.7	7.4×10^{-2}
aa1(1H$_2$O)m	2.39×10^2	18.6	1.3×10^{-1}	11.2	2.5×10^0	13.1	1.2×10^0	21.4	4.4×10^{-2}	10.5	3.3×10^0
aa1(2H$_2$O)	1.59×10^1	7.3	8.3×10^{-1}	−5.0	1.1×10^2	−1.5	2.8×10^1	3.4	4.0×10^0	−5.7	1.5×10^2
						Dimer					
aa2	1.42×10^2	24.8	6.6×10^{-3}	13.6	5.9×10^{-1}	17.5	1.2×10^{-1}	26.5	3.3×10^{-3}	16.3	1.9×10^{-1}
aa2(1H$_2$O)m	7.83×10^2	19.0	3.6×10^{-1}	10.3	1.2×10^1	13.0	4.1×10^0	16.5	1.0×10^0	8.7	2.3×10^1
aa2(2H$_2$O)	1.08×10^1	6.8	6.7×10^{-1}	−6.4	1.3×10^2	−2.7	3.1×10^1	−2.4	2.6×10^1	−8.6	3.3×10^2
						Trimer					
aa3	2.30×10^2	26.7	5.0×10^{-3}	15.6	4.3×10^{-1}	18.8	1.2×10^{-1}	25.4	8.3×10^{-3}	17.0	2.4×10^{-1}
aa3(1H$_2$O)m	1.10×10^2	20.1	3.3×10^{-2}	11.1	1.2×10^0	13.6	4.4×10^{-1}	13.6	4.6×10^{-1}	7.8	4.5×10^0
						Experimental Values					
ref 21	1.58×10^4	13.4	7.4×10^1								
ref 21	1.26×10^4	12.9	7.1×10^1								

[a] E_A is in kJ·mol^{-1}, A is in m^3.mol^{-1}.s^{-1}, hence k_{298K} is in mol.m^{-3}.s^{-1}.

Table 5. Kinetic Parameters for the Addition of Acrylamide to a Monomeric ($n = 1$), Dimeric ($n = 2$), or Trimeric ($n = 3$) Radical Chain for Different Levels of Solvation and Different Electronic Structure Methods Using the Implicit/Explicit Solvent Model[a]

	k_{298K}				
	B3LYP	MPWB1K	BMK	MP2	B2PLYP
			Monomer		
aa1	6.6×10^1	2.6×10^3	6.7×10^2	7.7×10^0	1.0×10^3
aa1(1H$_2$O)m	1.7×10^3	2.5×10^4	8.3×10^3	3.7×10^2	3.5×10^4
aa1(2H$_2$O)	3.9×10^1	2.8×10^3	5.9×10^2	3.7×10^2	4.4×10^3
			Dimer		
aa2	2.7×10^1	1.4×10^3	3.4×10^2	1.7×10^1	7.5×10^2
aa2(1H$_2$O)m	3.4×10^2	9.8×10^3	2.4×10^3	8.4×10^2	1.7×10^4
aa2(2H$_2$O)	1.8×10^1	2.5×10^3	3.7×10^2	1.4×10^3	4.8×10^3
			Trimer		
aa1	1.4×10^1	8.7×10^2	2.0×10^2	2.6×10^1	6.4×10^2
aa3(1H$_2$O)m	1.2×10^2	4.0×10^3	9.5×10^2	1.4×10^3	1.4×10^4
			Experimental Values		
ref 21	7.4×10^1				
ref 21	7.1×10^1				

[a] k_{298K} is in mol·m^{-3}·s^{-1}.

experimentally) is well reproduced by the MPWB1K, BMK, and B2PLYP methods in the continuum solvent model approach, yielding a ratio of 38, 71, and 94 respectively using the trimer radical (Table 8). None of the gas phase methods succeeds in reproducing this ratio properly. With B3LYP, the ratio is exhaustively too large giving values between 500 and 5000 both with and without implicit solvent model, indicating that this functional does not reproduce the qualitative features of the polymerization, as was earlier reported by Coote et al.[37]

From Table 4 and Table 6, the influence of adding explicit water molecules on the activation energy becomes very clear. Upon the addition of one or two water molecules, a significant decrease in activation energy is observed. Depending on the electronic level of theory the shift varies between 4 and 10 kJ/mol in case of one explicit water molecule. The main effect of the explicit water molecule is loosening the original intermolecular hydrogen bond between the amide hydrogen and the acrylic oxygen. This strong interaction forces the substituents about the forming bond to take an almost eclipsed configuration of 18° for AA and 5° for MAA (see Figure 8) in vacuo. In the presence of a water molecule, the angle between the substituents rises to 30° and 35°, respectively, causing structural relaxation. This results in an increase of the reaction rate coefficient, regardless of the electronic structure method or polymer model that is used.

Some activation energies turn out to become negative upon the addition of two water molecules and require some special attention. Because of the very high negative solvation energy, this transition state can become more stable than its reactants and the reaction can therefore exhibit a negative activation energy. This shows that the modeled reaction is not elementary, but a combination of two events: the formation of the prereactive complex (for which pseudo stationarity is assumed) and the unimolecular reaction transforming this complex into the products. This negative activation energy is a result of linearly fitting the natural logarithm of the obtained numbers for k_p against temperature inversed. At low temperatures, the relative importance of the PRC is higher and it can therefore have an influence on the reaction rate while at higher temperature, it is easily formed and the reaction itself is the only determining factor. For acrylamide, the trimeric model with 1 explicit water molecule (**aa3(1h2o)m**) gives results that lie very close to the experimental ones with the BMK, MPWB1K and B2-PLYP functional and the MP2 method. Especially the activation energy is in good agreement with the experimental value whereas the frequency factor is underestimated for the B3LYP geometries. The same is the case for MAA: although the better electronic structure methods yield activation energies that lie in the near vicinity of the experimental value, the reaction rate is underestimated. For the MAA monomer, the discrepancy is bigger than for AA. Rather than focusing solely on the quantitative agreement between calculated and experimental rate constants, it is more important to validate whether qualitative trends are reproduced. The AA/MAA rate ratios are shown in Table 8. The explicitly solvated trimeric model gives a AA/MAA ratio of 57 and 68 at the MPWB1K and BMK level of theory, which is in very good agreement with the experimental value of 67. B3LYP again significantly overestimates the ratio.

Table 6. Kinetic Parameters for the Addition of Methacrylamide to a Monomeric ($n = 1$), Dimeric ($n = 2$), or Trimeric ($n = 3$) Radical Chain for Different Levels of Solvation and Different Electronic Structure Methods[a]

	B3LYP			MPWB1K		BMK		MP2		B2PLYP	
	A	E_A	k_{298K}	E_A	k_{298K}	E_A	k_{298K}	E_A	k_{298K}	E_A	k_{298K}
					Monomer						
maa1	7.24×10^1	31.6	2.2×10^{-4}	15.9	1.2×10^{-1}	19.9	2.4×10^{-2}	19.6	2.6×10^{-2}	17.5	6.1×10^{-2}
maa1(1H$_2$O)m	1.78×10^1	27.7	2.6×10^{-4}	11.2	1.9×10^{-1}	14.2	5.7×10^{-2}	10.0	3.1×10^{-1}	10.8	2.3×10^{-1}
maa1(2H$_2$O)	1.65×10^0	17.8	1.3×10^{-3}	0.5	1.3×10^0	3.2	4.4×10^{-1}	−4.4	9.4×10^0	−3.0	5.2×10^0
					Dimer						
maa2	3.55×10^1	40.1	3.5×10^{-6}	17.9	2.6×10^{-2}	22.8	3.6×10^{-3}	18.9	1.7×10^{-2}	22.0	5.0×10^{-3}
maa2(1H$_2$O)m	1.04×10^1	36.0	5.4×10^{-6}	12.5	6.7×10^{-2}	16.6	1.3×10^{-2}	7.3	5.3×10^{-1}	14.1	3.5×10^{-2}
maa2(2H$_2$O)	1.29×10^0	28.1	1.6×10^{-5}	4.9	1.7×10^{-1}	8.1	4.8×10^{-2}	−3.9	5.9×10^0	3.0	3.7×10^{-1}
					Trimer						
maa3	5.33×10^1	42.1	2.4×10^{-6}	18.8	2.7×10^{-2}	23.6	3.9×10^{-3}	18.2	3.5×10^{-2}	22.6	5.9×10^{-3}
maa3(1H$_2$O)m	4.08×10^1	40.2	3.9×10^{-6}	18.8	2.1×10^{-2}	21.7	6.5×10^{-3}	13.2	2.0×10^{-1}	18.6	2.2×10^{-2}
					Experimental Values						
ref 29		20.0	1.1×10^0								

[a] E_A is in kJ·mol^{-1}, and A is in m^3·mol^{-1}·s^{-1}; hence, k_{298K} is in mol·m^{-3}·s^{-1}.

Table 7. Kinetic Parameters for the Addition of Methacrylamide to a Monomeric ($n = 1$), Dimeric ($n = 2$), or Trimeric ($n = 3$) Radical Chain for Different Levels of Solvation and Different Electronic Structure Methods Using the Implicit/Explicit Solvent Model[a]

	k_{300K}				
	B3LYP	MPWB1K	BMK	MP2	B2PLYP
			Monomer		
maa1	1.3×10^{-1}	7.0×10^1	9.2×10^0	1.5×10^1	3.9×10^1
maa1(1H$_2$O)m	2.2×10^{-1}	1.9×10^2	3.3×10^1	2.0×10^2	1.7×10^2
maa1(2H$_2$O)	2.7×10^{-3}	2.7×10^0	5.4×10^{-1}	4.4×10^1	8.0×10^0
			Dimer		
maa2	1.1×10^{-2}	5.8×10^1	6.7×10^0	6.0×10^1	1.5×10^1
maa2(1H$_2$O)m	5.2×10^{-3}	6.0×10^1	8.2×10^0	4.6×10^2	2.9×10^1
maa2(2H$_2$O)	8.0×10^{-7}	6.5×10^{-3}	1.1×10^{-3}	3.9×10^{-1}	1.2×10^{-2}
			Trimer		
maa3	2.6×10^{-3}	2.3×10^1	2.8×10^0	5.3×10^1	6.8×10^0
maa3(1H$_2$O)m	3.1×10^{-3}	1.5×10^1	3.5×10^0	1.7×10^2	1.5×10^1
			Experimental Values		
ref 29	1.1×10^0				

[a] k_{298K} is in mol·m^{-3}·s^{-1}.

Table 8. AA/MAA Rate Ratio for Addition to a Trimeric Radical in Vacuo, with 1 Explicit Water Molecule, in the Continuum Model and in the Combined Explicit/Implicit Solvation Model for All Studied Electronic Structure Methods[a]

	in vacuo		C-PCM	
	without H$_2$O	with 1 H$_2$O	without H$_2$O	with 1 H$_2$O
B3LYP	2083	8462	5385	38 710
MPWB1K	16	57	38	267
BMK	31	68	71	271
MP2	0	2	0	8
B2PLYP	41	205	94	933
experimental		67−75		

[a] The experimental range for this ratio is about 67−75.

The mixed implicit/explicit solvent model results, based on the free energy differences in solution, account for a major increase in the reaction rates of about 3 orders of magnitude. They largely overshoot the experimental values for acrylamide polymerization, while reproducing the MAA polymerization rate quite well. As a result the AA/MAA rate ratio is too large, giving values of around 270 at the best levels of theory. At first sight, the mixed solvation models give better results for the MAA polymerization system but these are probably due to a fortuitous cancellation of effects. An interesting study concerning the mixed solvation models was recently published by Warshel et al.[42] The reliability of the mixed solvation models is largely dependent on the conformations of the water molecules. There is no guarantee that the explicit water molecules have the correct orientation as they would have in an explicit infinite system, for instance reulting from QM/MM molecular dynamics runs. For the MAA polymerization system, the combination of a too low k_p prediction with explicit solvent molecules with an excessive effect of the C-PCM model on a system with explicit water molecules leads to a fairly good agreement with the experiment but this is due to a cancellation of errors.

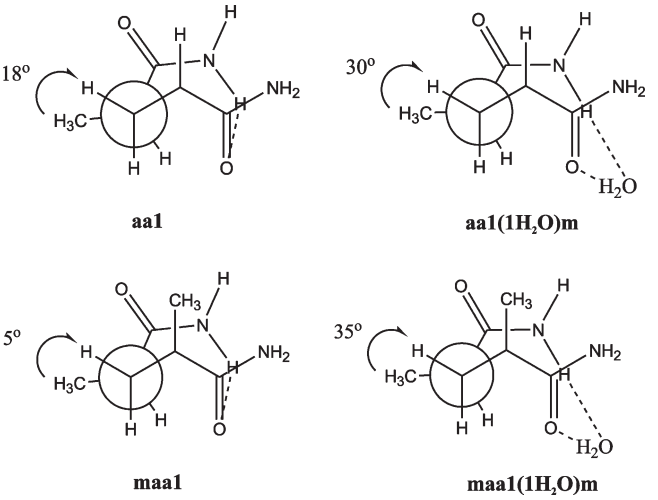

Figure 8. Newman projection along the forming bond for the acrylamide and methacrylamide monomeric transition states with 0 and 1 water molecule assisting.

Conclusion

The radical polymerization reaction for both acrylamide and methacrylamide was studied in the presence and absence of

explicit water molecules. The calculations reveal that an important solvent effect can be attributed to these solvent molecules, stabilizing the transition state and thereby lowering the activation energy of the reactions by 4−10 kJ/mol depending on the electronic structure method used. As the propagation rates were seriously underestimated when modeled in the gas phase, the inclusion of explicit water molecules brings the propagation rates much closer to the experimental values. The reaction rates also increase significantly by using an implicit solvent model. In general, gas phase calculations can give reliable and quite accurate activation energies when an appropriate description of the system is used in terms of electronic structure method and explicit solvation. A remaining challenge lies in a good description of the pre-exponential factor. More advanced techniques in which the solvent environment around the reactive center is taken into account entirely, so as to include all possible entropic contributions might contribute to a better description of the pre-exponential factor. Apart from the absolute comparison of calculated and experimental rate constants it is also very important to validate the relative rates of polymerization of the AA versus the MAA polymerization system. Experimentally, this ratio is estimated at 67. Simple gas phase calculations underestimate this ratio apart from B3LYP which gives unrealistically high results. The ratio is well reproduced when using the implicit or the explicit solvation model. The results of the mixed solvation model should be treated with care as the results are very much dependent on the position of the explicit solvent molecules. In general, the BMK and MPWB1K functionals give the best quantitative and qualitative picture for the trimeric model. These results are in agreement with the earlier work of Broadbelt and co-workers.[10]

Acknowledgment. The authors thank the FWO (Fonds voor Wetenschappelijk Onderzoek−Vlaanderen, Fund for Scientific Research−Flanders), the research board of Ghent University and the IAP-BELSPO project in the frame of IAP 6/27 for financial support of this research. Computational resources and services used in this work were provided by Ghent University.

Supporting Information Available: Tables of the *xyz* coordinates and energies of all structures. This material is available free of charge via the Internet at http://pubs.acs.org.

References and Notes

(1) Olaj, O. F.; Bitai, I.; Hinkelmann, F. *Makromol. Chem.* **1987**, *188*, 1689–1702.
(2) Olaj, O. F.; Schnollbitai, I. *Eur. Polym. J.* **1989**, *25*, 635–641.
(3) Van Herk, A. M. *Macromol. Theor. Simul.* **2000**, *9*, 433–441.
(4) Beuermann, S.; Buback, M. *Prog. Polym. Sci.* **2002**, *27*, 191–254.
(5) Barner-Kowollik, C.; Buback, M.; Egorov, M.; Fukuda, T.; Goto, A.; Olaj, O. F.; Russell, G. T.; Vana, P.; Yamada, B.; Zetterlund, P. B. *Prog. Polym. Sci.* **2005**, *30*, 605–643.
(6) Van Cauter, K.; Van Speybroeck, V.; Vansteenkiste, P.; Reyniers, M. F.; Waroquier, M. *ChemPhysChem* **2006**, *7*, 131–140.
(7) Van Cauter, K.; Hemelsoet, K.; Van Speybroeck, V.; Reyniers, M. F.; Waroquier, M. *Int. J. Quantum Chem.* **2005**, *102*, 454–460.
(8) Degirmenci, I.; Avci, D.; Aviyente, V.; Van Cauter, K.; Van Speybroeck, V.; Waroquier, M. *Macromolecules* **2007**, *40*, 9590–9602.
(9) Degirmenci, I.; Aviyente, V.; Van Speybroeck, V.; Waroquier, M. *Macromolecules* **2009**, *42*, 3033–3041.
(10) Yu, X. R.; Pfaendtner, J.; Broadbelt, L. J. *J. Phys. Chem. A* **2008**, *112*, 6772–6782.
(11) Thickett, S. C.; Gilbert, R. G. *Macromolecules* **2008**, *41*, 4528–4530.
(12) Huang, D. M.; Monteiro, M. J.; Gilbert, R. G. *Macromolecules* **1998**, *31*, 5175–5187.
(13) Van Cauter, K.; Van Speybroeck, V.; Waroquier, M. *ChemPhysChem* **2007**, *8*, 541–552.
(14) Olaj, O. F.; Schnoll-Bitai, I. *Monatsh. Chem.* **1999**, *130*, 731–740.
(15) Beuermann, S. *Macromol. Rapid Commun.* **2009**, *30*, 1066–1088.
(16) Beuermann, S.; Garcia, N. *Macromolecules* **2004**, *37*, 3018–3025.
(17) O'driscoll, K. F.; Monteiro, M. L.; Klumperman, B. *J. Polym. Sci. A* **1997**, *35*, 515–520.
(18) Zammit, M. D.; Davis, T. P.; Willett, G. D.; Odriscoll, K. F. *J. Polym. Sci. A* **1997**, *35*, 2311–2321.
(19) Beuermann, S. *Macromolecules* **2004**, *37*, 1037–1041.
(20) Lin, H. R. *Eur. Polym. J.* **2001**, *37*, 1507–1510.
(21) Seabrook, S. A.; Tonge, M. P.; Gilbert, R. G. J. *Polym. Sci. A* **2005**, *43*, 1357–1368.
(22) Jiang, Y.; Garland, M.; Carpenter, K. J.; Suresh, P. S.; Widjaja, E. *J. Polym. Sci. A* **2007**, *45*, 5697–5704.
(23) Ganachaud, F.; Balic, R.; Monteiro, M. J.; Gilbert, R. G. *Macromolecules* **2000**, *33*, 8589–8596.
(24) Kuchta, F. D.; van Herk, A. M.; German, A. L. *Macromolecules* **2000**, *33*, 3641–3649.
(25) Lacik, I.; Beuermann, S.; Buback, M. *Macromolecules* **2003**, *36*, 9355–9363.
(26) Beuermann, S.; Paquet, D. A.; McMinn, J. H.; Hutchinson, R. A. *Macromolecules* **1997**, *30*, 194–197.
(27) Kamachi, M. *Adv. Polym. Sci.* **1987**, *82*, 207–275.
(28) Pascal, P.; Winnik, M. A.; Napper, D. H.; Gilbert, R. G. *Macromolecules* **1993**, *26*, 4572–4576.
(29) Pascal, P.; Napper, D. H.; Gilbert, R. G.; Piton, M. C.; Winnik, M. A. *Macromolecules* **1990**, *23*, 5161–5163.
(30) Seabrook, S. A.; Gilbert, R. G. *Polymer* **2007**, *48*, 4733–4741.
(31) Thiel, J.; Maurer, G.; Prausnitz, J. M. *Chem.-Ing.-Tech.* **1995**, *67*, 1567–1583.
(32) Fernandez-Barbero, A.; Suarez, I. J.; Sierra-Martin, B.; Fernandez-Nieves, A.; de las Nieves, F. J.; Marquez, M.; Rubio-Retama, J.; Lopez-Cabarcos, E. *Adv. Colloid Interface Sci.* **2009**, *147−48*, 88–108.
(33) Seelert, H.; Krause, F. *Electrophoresis* **2008**, *29*, 2617–2636.
(34) Aparicio-Martinez, A.; Hall, K. R.; Balbuena, P. B. *J. Phys. Chem. A* **2006**, *110*, 9183–9193.
(35) Aparicio-Martinez, S.; Balbuena, P. B. *Mol. Simulat.* **2007**, *33*, 925–938.
(36) Barabanova, A. I.; Bune, E. V.; Gromov, A. V.; Gromov, V. F. *Eur. Polym. J.* **2000**, *36*, 479–483.
(37) Izgorodina, E. I.; Coote, M. L. *Chem. Phys.* **2006**, *324*, 96–110.
(38) Thickett, S. C.; Gilbert, R. G. *Polymer* **2004**, *45*, 6993–6999.
(39) Pliego, J. R.; Riveros, J. M. *J. Phys. Chem. A* **2001**, *105*, 7241–7247.
(40) Kelly, C. P.; Cramer, C. J.; Truhlar, D. G. *J. Phys. Chem. A* **2006**, *110*, 2493–2499.
(41) da Silva, E. F.; Svendsen, H. F.; Merz, K. M. *J. Phys. Chem. A* **2009**, *113*, 6404–6409.
(42) Kamerlin, S. C. L.; Haranczyk, M.; Warshel, A. *ChemPhysChem* **2009**, *10*, 1125–1134.
(43) Heuts, J. P. A.; Gilbert, R. G.; Radom, L. *Macromolecules* **1995**, *28*, 8771–8781.
(44) Heuts, J. P. A.; Gilbert, R. G.; Radom, L. *J. Phys. Chem.* **1996**, *100*, 18997–19006.
(45) Zetterlund, P. B.; Busfield, W. K.; Jenkins, I. D. *Macromolecules* **1999**, *32*, 8041–8045.
(46) De Sterck, B.; Van Speybroeck, V.; Mangelinckx, S.; Verniest, G.; De Kimpe, N.; Waroquier, M. *J. Phys. Chem. A* **2009**, *113*, 6375–6380.
(47) Van Speybroeck, V.; Moonen, K.; Hemelsoet, K.; Stevens, C.; Waroquier, M. *J. Am. Chem. Soc.* **2006**, *128*, 8468–8478.
(48) Manukyan, A. K.; Radkiewicz-Poutsma, J. L. *J. Mol. Struct.—THEOCHEM* **2006**, *766*, 105–112.
(49) Kelly, C. P.; Cramer, C. J.; Truhlar, D. G. *J. Chem. Theory Comput.* **2005**, *1*, 1133–1152.
(50) Takano, Y.; Houk, K. N. *J. Chem. Theory Comput.* **2005**, *1*, 70–77.
(51) Frisch, M. J. et al.et al. *Gaussian 03, Revision C.02*; Gaussian, Inc.: Wallingford, CT, 2004.
(52) Becke, A. D. *J. Chem. Phys.* **1993**, *98*, 5648–5652.
(53) Lee, C. T.; Yang, W. T.; Parr, R. G. *Phys. Rev. B* **1988**, *37*, 785–789.
(54) Zhao, Y.; Truhlar, D. G. *J. Phys. Chem. A* **2004**, *108*, 6908–6918.
(55) Boese, A. D.; Martin, J. M. L. *Abstracts of Papers, 229th National Meeting of the American Chemical Society, San Diego, CA*; American Chemical Society: Washington, DC, 2005; p 274-COMP.
(56) Hemelsoet, K.; Van Speybroeck, V.; Waroquier, M. *J. Phys. Chem. A* **2008**, *112*, 13566–13573.
(57) Becke, A. D. *Phys. Rev. A* **1988**, *38*, 3098–3100.
(58) Grimme, S. *J. Chem. Phys.* **2006**, *124*, 034108.
(59) Korth, M.; Grimme, S. *J. Chem. Theory Comput.* **2009**, *5*, 993–1003.
(60) Bennaim, A. *J. Chem. Phys.* **1990**, *93*, 8196–8210.
(61) Singleton, D. L.; Cvetanovic, R. J. *J. Am. Chem. Soc.* **1976**, *98*, 6812–6819.
(62) Van Cauter, K.; Van den Bossche, B. J.; Van Speybroeck, V.; Waroquier, M. *Macromolecules* **2007**, *40*, 1321–1331.